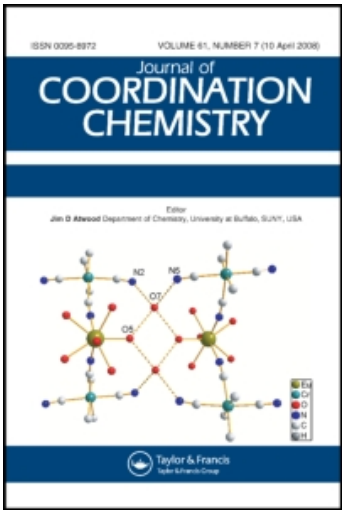

Journal of Coordination Chemistry
Publication details, including instructions for authors and subscription information:
http://www.informaworld.com/smpp/title~content=t713455674

Structural and Anion Coordination Features of Macrocyclic Polyammonium Cations in the Solid, Solution and Computational Phases

Stéphane Boudon[a]; André Decian[a]; Jean Fischer[a]; Wais Hosseini[a]; Jean-Marie Lehn[a]; Georges Wipff[a]
[a] Institut Le Bel, Université Louis Pasteur, Strasburg, France

To cite this Article Boudon, Stéphane , Decian, André , Fischer, Jean , Hosseini, Wais , Lehn, Jean-Marie and Wipff, Georges(1991) 'Structural and Anion Coordination Features of Macrocyclic Polyammonium Cations in the Solid, Solution and Computational Phases', Journal of Coordination Chemistry, 23: 1, 113 — 135
To link to this Article: DOI: 10.1080/00958979109408246
URL: http://dx.doi.org/10.1080/00958979109408246

J. Coord. Chem. 1991, Vol. 23. pp. 113–135
Reprints available directly from the publisher
Photocopying permitted by license only

STRUCTURAL AND ANION COORDINATION FEATURES OF MACROCYCLIC POLYAMMONIUM CATIONS IN THE SOLID, SOLUTION AND COMPUTATIONAL PHASES

STÉPHANE BOUDON, ANDRÉ DECIAN, JEAN FISCHER, MIR WAIS HOSSEINI, JEAN-MARIE LEHN* and GEORGES WIPFF

Institut Le Bel, Université Louis Pasteur, 4 rue Blaise Pascal, 67000 Strasbourg, France

(Received July 27, 1990)

The crystal structures of two hexaaza macrocycles 1,4,7,12,15,18-hexaazacyclodocosane ([22]N_6:**1**-6H^+, 6Cl^-) and 1,13-dioxa-4,7,10,16,19,22-hexaazacyclotetraeicosane ([24]N_6O_2:**2**-6H^+,6Cl^-) as their hexahydrochloride salts have been determined. **1**-6H^+ binds specifically two Cl^- anions above and below the almost planar hexaammonium macrocycle yielding a dinuclear Cl^- complex. The hexacation **2**-6H^+ on the other hand interacts preferentially with three Cl^- anions of the six present in the solid state. Among the three closest anions, one of them, interacting with four ammonium groups, is located in the centre of the macrocycle which adopts a "pocket-like" conformation. Potentiometric and ^{35}Cl NMR experiments demonstrate that **2**-6H^+ also binds Cl^- in aqueous solution. Subsequent extensive molecular dynamics computational studies starting from X-ray coordinates show that the solid state structure is representative of the solution conformations for **1**-6H^+, whereas the conformations of **2**-6H^+ are strongly affected by intramolecular interactions between the ammonium centres and O-atoms of the ether linkage as well as by intermolecular interactions with H_2O molecules and Cl^- counterions.

Keywords: Polyammonium macrocycles, dinuclear chloride complex, molecular dynamics

INTRODUCTION

Anions play important roles in both chemical and biochemical processes.[1] Anion coordination chemistry, *i.e.* binding of negatively charged substrates by organic receptor molecules has recently been recognized and developed as a new area of coordination chemistry[2] (for reviews see ref. 3). Synthetic receptor molecules containing amine functionalities are particularly interesting ligands, since, they either bind transition metals[4] when unprotonated, or when protonated, anions by electrostatic interactions and H-bonding between their positively charged ammonium sites and negatively charged centres of anions.[3]

Macro(poly)cyclic polyamines, depending on their size and the location of their binding sites, form a variety of mono-, di- and polynuclear complexes with transition metal cations.[5] On the other hand, protonated polyamines bind organic,[6] inorganic[7–9] as well as biologically important anions.[10] Furthermore, partial protonation of polyamines leads to the formation of mixed complexes with simultaneous binding of transition metal cations and anions.[11]

Compounds **1**[12,13] and **2**[14] are 22 and 24 membered hexaaza ditopic macrocycles

* Author for correspondence.

incorporating two diethylenetriamine subunits. Whereas for macrocycle **1**, the two subunits are bridged by tetramethylene chains $(CH_2)_4$, in compound **2**, the spacers are two $CH_2CH_2OCH_2CH_2$ fragments. In the latter case, although the presence of an O-atom in position 3 with respect to an N-atom, lowers the protonation constants, the $CH_2CH_2OCH_2CH_2$ unit may induce solution conformations of the protonated macrocycle more adaptable for encircling the bound anion. Furthermore, electrostatic N^+–H···O interactions may also lead to some structure holding in solution.

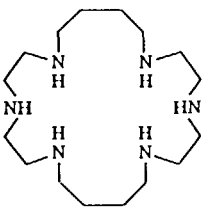

1

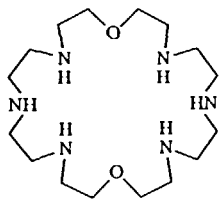

2

Among various polyamines investigated, the ditopic macrocyclic hexaamine **2** has been shown to illustrate nicely this dual ability to bind both cations and anions. Indeed, whereas unprotonated **2** yields dinuclear Cu,[14–16] Ni,[16] Co[16,17] and Rh[18] complexes, its protonated form leads in aqueous solution to a variety of stable complexes with nucleotides and polyphosphates with marked selectivity.[10] Moreover, protonated **2** catalyses the hydrolysis of nucleotide polyphosphates,[19] as well as phosphorylation processes in phosphate and phosphate-containing biologically important substrates.[13,20]

Many crystal structures are available for macrocyclic transition metal complexes, in particular for compound **2**.[14,15,18] However, only a few structures have been reported for anion binding by macrocyclic polyammonium cations.[21–25] Most studies concern the complexation of halide ions, in particular Cl^-, by protonated macro-bicyclic and -tricyclic polyamines[7,21–23] both in solution and in the solid state. The only example of Cl^- binding by a macromono-cyclic polycationic receptor was reported for the tetraprotonated hexaamine [18]N_6 as its dichloride-dinitrate salt. In this case, the X-ray study indicated that both Cl^- anions, located below and above the plane of the macrocycle, were intermolecularly coordinated to two macrocycles.[24]

We report here the solid state structures of the hydrochloride salts of the fully protonated hexaazamacrocycles **1** and **2**, the binding ability of protonated **2** towards Cl^- anion in solution as well as computer modelling studies of protonated **1** and **2** in a continuous dielectric medium and in water with or without counter-ions by means of molecular dynamics calculations.

Crystal Structures of 1-6H^+,6Cl^-,2H_2O and 2-6H^+,6Cl^-,4H_2O

X-Ray Diffraction Experiments

Suitable single crystals of 1-6HCl and 2-6HCl were obtained by slow liquid–liquid diffusion of, respectively, MeOH and 2-propanol into water at room temperature. Systematic searches in reciprocal space using a Philips PW1100/16 automatic diffractometer showed that crystals of **1** and **2** belong to the monoclinic system.

Quantitative data were obtained at −100°C using a locally built gas flow device. All experimental parameters used are given in Table I. The resulting data sets were transferred to a VAX computer, and for all subsequent calculations a local data reduction program was used. Three standard reflections were measured every hour during the entire data acquisition periods and showed no significant trend. The raw step-scan data were converted to intensities using the Lehmann-Larsen method[27] and then corrected for Lorentz and polarization factors.

TABLE I
X-ray diffraction experimental parameters.

Formula	$C_{16}H_{48}N_6O_2Cl_6$	$C_{16}H_{52}N_6O_6Cl_6$
Molecular weight	569.32	637.35
Colour	none	none
Crystal System	Monoclinic	Monoclinic
a (Å)	7.553(4)	22.178(5)
b (Å)	7.098(2)	10.759(3)
c (Å)	11.235(3)	12.924(3)
β (deg)	91.79(2)	97.01(2)
U (Å^3)	1399.1	3060.8
Z	2	4
Dcalc (gcm^{-1})	1.1.351	1.383
Space group	$P2_1/n$	$P2_1/c$
Radiation	CuK_α(graphite mono λ)	
Wavelength (Å)	1.5418	1.5418
μ(cm^{-1})	59.373	55.815
Crystal size (mm)	0.30 × 0.14 × 0.07	0.22 × 0.30 × 0.40
Temperature	−100°C	−100°C
Diffractometer	Philips PW1100/16	
Mode	θ/2θ flying step-scan	
Scan speed (deg^{-1})	0.020	0.024
Scan width (deg)	0.90 + 0.143tg(θ)	1.00 + 0.143tg(θ)
Step width (deg)	0.05	0.05
Theta limits (deg)	3/51	3–51
Octants	$\pm h + k + l$	$\pm h + k + l$
Number of data collected	1678	3683
Number of data with $I > 3\sigma(I)$	1232	3225
Abs. min/max	0.75/1.19	0.85/1.27
$R(F)$	0.030	0.047
$R_w(F)$	0.055	0.090
p	0.08	0.08
GOF	1.28	1.97

The structures were solved using MULTAN.[28] After refinement of the heavy atoms, a difference-Fourier map revealed maxima of residual electronic density close to the positions expected for hydrogen atoms; they were introduced in structure factor calculations with computed coordinates (C–H = N–H = 0.95 Å) and isotropic temperature factors such as B(H) = 1.3 × Beqv(C/N) Å^2, but not refined. Since in the cold gas stream, face indexation was not possible, empirical absorption corrections were applied using the method of Walker and Stuart.[29] Final difference maps revealed no significant maxima. The scattering factor and anomalous dispersion coefficients were taken from International Tables for X-ray Crystallography.[30]

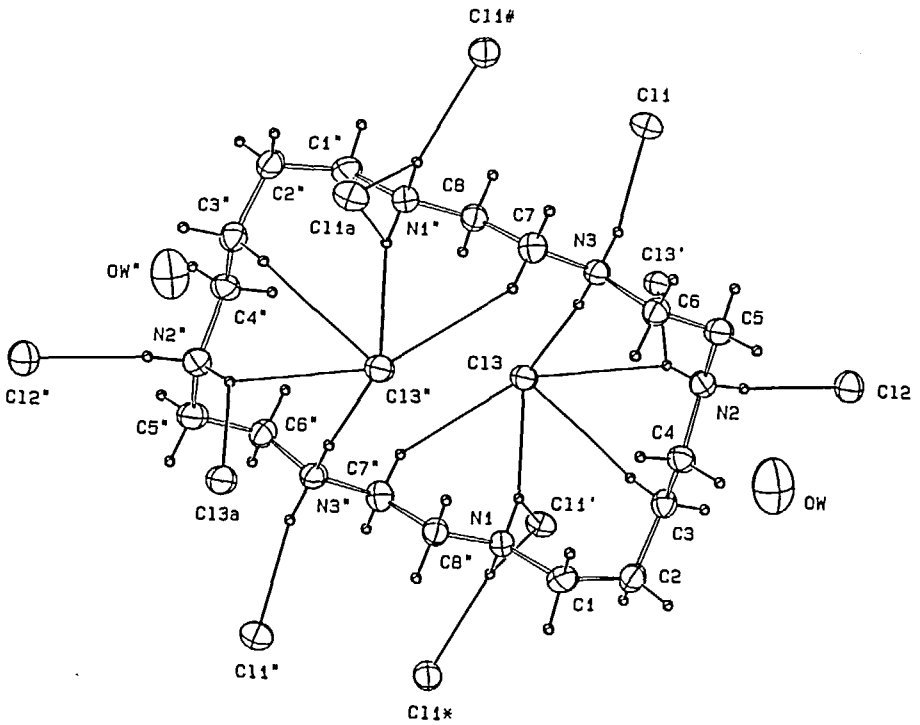

FIGURE 1 The structure of the 1-6H$^+$ macrocycle and its environment in the crystal.

TABLE II
Positional parameters and E.S.D.'s for 1-6H$^+$,6Cl$^-$,2H$_2$O.

Atom	*x/a*	*y/b*	*z/c*	B(Å^2)
Cl1	−0.22237(5)	0.4617(1)	1.17631(7)	2.49(2)
Cl2	−0.12068(5)	0.0885(1)	0.67536(8)	2.76(2)
Cl3	0.03349(4)	0.7272(1)	0.97544(7)	2.31(2)
OW	−0.1954(2)	0.7321(4)	0.5334(3)	5.24(8)
N1	0.1202(2)	0.9061(4)	0.7653(2)	1.96(6)
N2	−0.0879(2)	0.4738(4)	0.7876(2)	2.10(6)
N3	−0.1413(2)	0.7161(4)	1.0007(2)	2.04(6)
C1	0.0751(2)	0.8881(5)	0.6500(3)	2.44(8)
C2	0.0718(2)	0.6879(6)	0.6044(3)	2.44(8)
C3	0.0300(2)	0.5470(5)	0.6822(3)	2.19(8)
C4	−0.0518(2)	0.6020(5)	0.6998(3)	2.31(8)
C5	−0.1676(2)	0.5207(6)	0.8184(3)	2.43(8)
C6	−0.1786(2)	0.7073(5)	0.8788(3)	2.20(8)
C7	−0.1577(2)	0.8983(5)	1.0621(3)	2.34(8)
C8	−0.1118(2)	0.9058(5)	1.1785(3)	2.13(8)

Anisotropically refined atoms are given in the form of the isotropic equivalent displacement parame defined as: $(4/3)[a^2\beta(1,1) + b^2\beta(2,2) + c^2\beta(3,3) + ab(\cos\gamma)\beta(1,2) + ac(\cos\beta)\beta(1,3) + bc(\cos\alpha)\beta(2,3)]$

Structure of the Protonated Polyamines and Anion Coordination in the Solid State

In the solid state, **1**-6H$^+$ consisted of three discrete moieties: the 22 membered ring hexacation $[C_{16}H_{44}N_6]^{6+}$, 6 Cl^- anions and two H_2O molecules (Figure 1). Table II gives the relative coordinates and equivalent temperature factors of all independent non-hydrogen atoms. All atoms of the moieties are related two by two by a crystallographic inversion centre, thus only half of the atoms are independent. The **1**-6H$^+$ ring displays a nice rectangular shape based on a zigzag chain of N–C–C and C–C–C units with a sheet conformation. The overall almost planar shape of **1**-6H$^+$ is achieved by consecutive *trans* dihedral angles, with "corners" composed of two successive ($+g+g$ or $-g-g$) and alternating couples ($++--++--$) of dihedral angles (Figure 2). Two successive *gauche* dihedrals of the same orientation leading to a convergent change in direction of bonds achieved ring closure. Table III gives the dihedral angles of **1**-6H$^+$. The chloride ions Cl1 and Cl2 as well as the H_2O molecule are located around the ring, whereas the Cl3 anions are above and below the sheet (Figure 3).

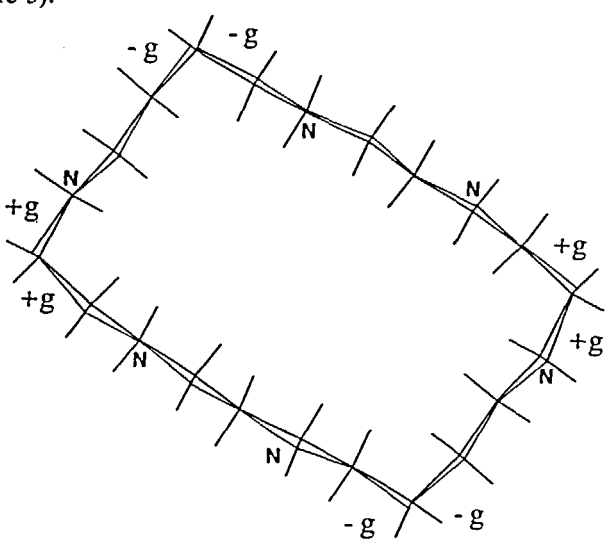

FIGURE 2 Conformations of the **1**-6H$^+$ macrocycle and its environment in the crystal.

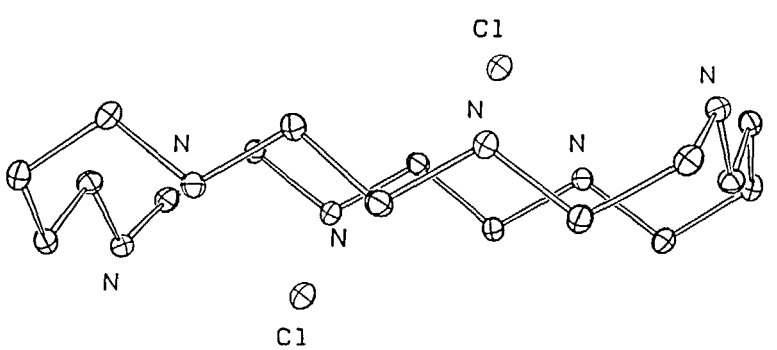

FIGURE 3 Location of Cl^- ions above and below the mean plane of the **1**-6H$^+$ macrocycle in the crystal.

TABLE III
Torsional angles in **1**-6H$^+$.

Atom 1	Atom 2	Atom 3	Atom 4	Angle (deg)
C5	N2	C4	C3	176.46 (0.28)
N1	C1	C2	C3	64.58 (0.39)
C4	N2	C5	C6	−63.17 (0.38)
C1	C2	C3	C4	59.17 (0.41)
C7	N3	C6	C5	−176.05 (0.28)
C2	C3	C4	N2	−173.33 (0.28)
C6	N3	C7	C8	−174.18 (0.27)
N2	C5	C6	N3	−66.04 (0.38)

All protonated amine sites have one proton turned inward, towards the centre of the ring. N1, N2, and N3 have one of the H-bonding sites turned below the mean plane of the cycle interacting with a specific Cl^- anion (C13). On the other hand, due to the symmetry of the crystal, protons belonging to the three other equivalent ammonium sites (N1″, N2″ and N3″) point in the opposite direction (above), interacting with the equivalent Cl^- anion (C13″). The three independent protonated amino groups do not have the same environment: N1 is linked *via* hydrogen bonds to chlorides Cl1′, Cl1* and Cl3, whereas N1, N2 are bound to three anions: Cl2, Cl3 and Cl3′; on the other hand N3 is linked to only two chlorides, Cl1 and Cl3. Cl1 has 4 contacts less than 3.5 Å: one with N3 of one ring, two with N1 of two other rings, and one with a water molecule. C12 is involved in only two contacts shorter than 3.5 Å: one with N2 of the independent ring and one with a water molecule. C13 has 6 contacts below 3.5 Å: only one of these contacts involves the ammonium group N2 of another ring. Thus C11 and C12 are involved in both intra- and intermolecular contacts, whereas C13 is mainly involved in intramolecular contacts. The water molecules have only two contacts less than 3.5 Å, as already described. Table IV summarizes these distances.

TABLE IV
N···Cl, N···water, water···Cl and Cl···Cl contacts of less than 3.5 Å in compound **1**-6H$^+$,6Cl$^-$,2H$_2$O. Starred value for intermolecular contacts.

N1···Cl1	3.112	N3···Cl1	3.058
N1···Cl3	3.120	N3···Cl3	3.091
N1···Cl1	3.223	Cl1···OW	3.175*
N2···Cl2	3.059	Cl2···OW	3.245
N2···Cl3	3.142	Cl3···Cl3	3.482
N2···Cl3	3.456		

In the solid state, **2**-6H$^+$ consisted of a 24-membered ring hexacation $[C_{16}H_{48}O_2N_6]^{6+}$, 6 chloride anions and 4 water molecules of crystallization. Figure 4 shows the cation together with the 6 Cl^- anions and H_2O molecules as well as the labelling scheme used. Table V lists atomic coordinates of all non-hydrogen atoms. Figure 5 shows a lateral view of the polycation **2**-6H$^+$, the anions and the water molecules. In the solid state **2**-6H$^+$ possesses a pocket-like conformation with the oxygen atoms O1 and O2 of the ring above the mean plane of the nitrogen atoms.

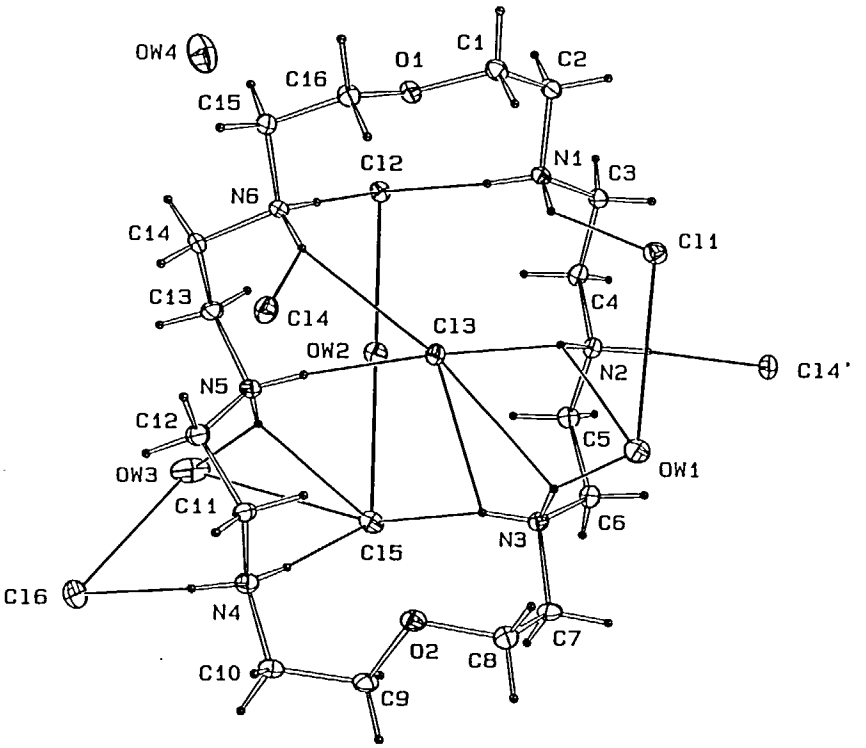

FIGURE 4 The structure of the 2-6H$^+$ macrocycle and its environment in the crystal.

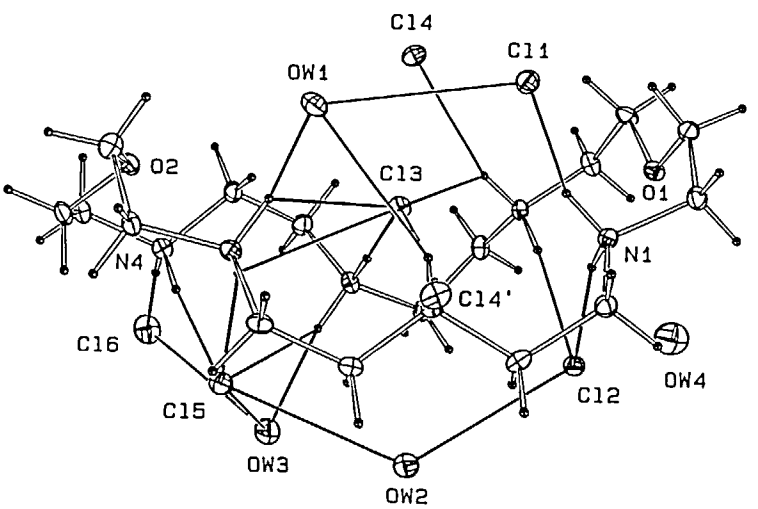

FIGURE 5 The 2-6H$^+$ macrocycle and its environment in the crystal; lateral view.

TABLE V
Positional parameters and E.S.D.'s for **2**-6H$^+$,6Cl$^-$,4H$_2$O.

Atom	*x/a*	*y/b*	*z/c*	B(Å^2)
Cl1	0.11323(4)	0.10671(8)	0.84823(7)	2.37(2)
Cl2	0.86282(4)	0.09041(8)	0.42577(7)	2.26(2)
Cl3	0.22645(4)	0.10745(8)	0.39232(7)	2.15(2)
Cl4	0.80278(4)	0.06548(8)	0.86874(7)	2.62(2)
Cl5	0.38212(4)	0.03188(9)	0.56380(7)	2.89(2)
Cl6	0.53635(5)	0.1663(1)	0.11486(9)	4.09(2)
O1	0.9544(1)	0.0152(2)	0.6458(2)	2.15(5)
C1	0.9846(2)	−0.1020(3)	0.6563(3)	2.23(8)
C2	0.9766(2)	−0.1616(3)	0.5509(3)	2.28(7)
N1	0.9105(1)	−0.1717(3)	0.5132(2)	1.86(6)
C3	0.8981(2)	−0.2437(3)	0.4135(3)	2.10(7)
C4	0.8335(2)	−0.2330(3)	0.3653(3)	2.25(7)
N2	0.7881(1)	−0.2962(3)	0.4268(2)	1.98(6)
C5	0.7263(2)	−0.2777(3)	0.3748(3)	2.24(7)
C6	0.6781(2)	−0.3500(3)	0.4217(3)	2.27(7)
N3	0.6649(1)	−0.3036(3)	0.5256(2)	1.96(6)
C7	0.6086(2)	−0.3602(4)	0.5574(3)	2.44(8)
C8	0.6010(2)	−0.3275(4)	0.6678(3)	2.84(8)
O2	0.5984(1)	−0.1965(2)	0.6854(2)	2.37(5)
C9	0.5401(2)	−0.1430(4)	0.6504(3)	2.60(8)
C10	0.5390(2)	−0.0121(4)	0.6904(3)	2.52(8)
N4	0.5852(1)	0.0686(3)	0.6492(2)	2.39(6)
C11	0.6447(2)	0.0755(3)	0.7163(3)	2.33(7)
C12	0.6842(2)	0.1820(4)	0.6891(3)	2.50(8)
N5	0.7129(1)	0.1571(3)	0.5925(2)	2.25(6)
C13	0.7573(2)	0.2548(3)	0.5674(3)	2.41(8)
C14	0.8114(2)	0.2721(3)	0.6477(3)	2.28(7)
N6	0.8511(1)	0.1596(3)	0.6604(2)	1.89(6)
C15	0.9116(2)	0.1873(3)	0.7197(3)	2.42(8)
C16	0.9467(2)	0.0707(4)	0.7435(3)	2.25(8)
OW1	0.2514(1)	0.4396(2)	0.3547(2)	2.84(5)
OW2	0.2700(1)	0.5620(3)	0.1761(2)	3.08(6)
OW3	0.3811(1)	0.7736(3)	0.0626(3)	4.98(8)
OW4	0.9369(2)	0.3932(4)	0.5152(3)	6.30(9)

Anisotropically refined atoms are given in the form of the isotropic equivalent displacement parameter defined as: $(4/3)[a^2\beta(1,1) + b^2\beta(2,2) + c^2\beta(3,3) + ab(\cos\gamma)\beta(1,2) + ac(\cos\beta)\beta(1,3) + bc(\cos\alpha)\beta(2,3)]$

The O–C–C–N$^+$ dihedral angles are all *gauche*, although not all are equivalent, three of them being $+g$ and one $-g$. $^+$N–C–C–N$^+$ dihedral angles are all in the *gauche* conformation equally distributed between $+g$ and $-g$ (Figure 6). Table VI lists the dihedral angles of **2**-6H$^+$. Each proton of the 6 nitrogen atoms is involved in short contacts with Cl$^-$ anions and/or water molecules and consequently each Cl$^-$ anion and water molecule has a lattice of short contacts (Table VII). Most of the protons of the 6 ammonium groups are turned toward the center of the "pocket". One of the protons of N2 and N4 interacts respectively with C16 and C16′. One chloride ion, C13 is bound by 4 ammonium groups with N $\cdots$ Cl$^-$ distances of less than 3.4 Å, and positioned in the centre of the pocket (Figure 7). The unsymmetrical shape of the

2-6H$^+$ molecule, however, indicates that it is not strictly a chloride receptor complementary to the spherical substrate.

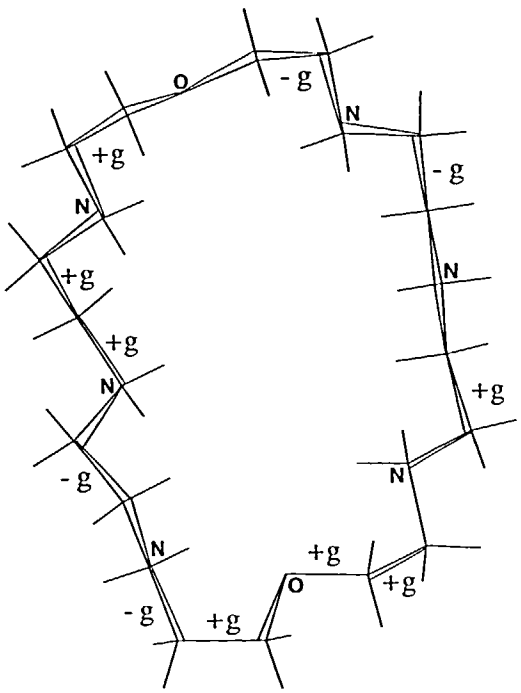

FIGURE 6 Conformations of the **2**-6H$^+$ macrocycle in the crystal.

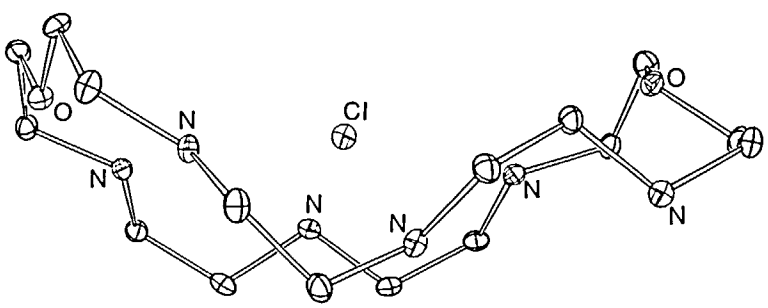

FIGURE 7 The **2**-6H$^+$ macrocycle and the centrally bound Cl^- anion in the crystal.

Binding Studies in Solution

pH-metric Measurements

Since polyamines bind anionic substrates only when protonated, the association constants are often experimentally determined by potentiometric methods. During pH-metric investigation of the complexation ability of macrocyclic polyamines

TABLE VI
Torsional angles in $2\text{-}6H^+$.

Atom 1	Atom 2	Atom 3	Atom 4	Angle (deg)
C16	O1	C1	C2	167.10 (0.28)
C7	C8	O2	C9	79.07 (0.37)
C1	O1	C16	C15	−176.64 (0.27)
C8	O2	C9	C10	169.50 (0.29)
O1	C1	C2	N1	−56.86 (0.35)
O2	C9	C10	N4	62.26 (0.39)
C1	C2	N1	C3	−173.35 (0.28)
C9	C10	N4	C11	−92.47 (0.37)
C2	N1	C3	C4	−168.91 (0.28)
C10	N4	C11	C12	−164.55 (0.30)
N1	C3	C4	N2	−68.23 (0.37)
N4	C11	C12	N5	−75.70 (0.38)
C3	C4	N2	C5	178.50 (0.29)
C11	C12	N5	C13	−174.55 (0.29)
C4	N2	C5	C6	172.69 (0.28)
C12	N5	C13	C14	61.68 (0.39)
N2	C5	C6	N3	71.32 (0.39)
N5	C13	C14	N6	64.13 (0.39)
C5	C6	N3	C7	167.84 (0.30)
C13	C14	N6	C15	165.95 (0.29)
C6	N3	C7	C8	171.68 (0.30)
C14	N6	C15	C16	172.32 (0.29)
N3	C7	C8	O2	58.28 (0.40)
N6	C15	C16	O1	60.44 (0.36)

TABLE VII
N···Cl, N···water, and water···Cl contacts less than 3.5 Å in $2\text{-}6H^+,6Cl^-,4H_2O$. Starred values are intermolecular contacts.

N1···Cl1	3.066	N5···Cl5	3.408
N1···Cl2	3.171	N6···Cl2	3.164
N1···Cl3	3.479	N6···Cl4	3.182
N2···Cl4	3.020*	N6···I13	3.375
N2···Cl3	3.143	OW1···OW2	2.732*
N2···OW1	3.425	OW1···Cl1	3.096
N3···OW1	2.698	OW2···Cl2	3.092
N3···Cl5	3.267	OW2···Cl5	3.191
N3···Cl3	3.280	OW2···Cl2	3.350*
N4···Cl6	3.064	OW3···Cl6	3.172
N4···Cl5	3.125	OW3···Cl5	3.286
N5···OW3	2.985	OW4···Cl1	3.179*
N5···Cl3	3.144	OW4···Cl4	3.355*

toward anions, we previously noticed that these protonated compounds bind to some extent the anion of the supporting electrolyte such as NMe_4Cl.[31,32] Indeed, the protonation constants $\log K_n$ (pK_n values) corresponding to the equilibrium equations (*1*) and (*2*) of the polyamine (L = **2**) were significantly different in the presence of NMe_4Cl and sodium *para*-toluene sulfonate (TsONa).

$$H_{n-1}L^{(n-1)+} + H^+ \rightleftharpoons H_nL^{n+} \quad (1)$$

$$K_n = [H_nL^{n+}]/[H_{n-1}L^{(n-1)+}][H^+] \quad (2)$$

The pK_i values (i = 1–6) (in aqueous solution at 25°C) were found to be 9.15, 9.00, 8.20, 7.20, 3.70 and 3.40 in the presence of 0.1 M TsONa[31] and 9.60, 9.35, 8.30, 8.10, 4.00 and 3.80 in the presence of 0.1 M NMe_4Cl[32]. It may be noticed that the pK_i values for the tetra-(pK_4), penta-(pK_5) and hexaprotonated (pK_6) forms of **2** were substantially higher in the presence of Cl^- than in the presence of TsO^-, indicating a stronger binding of chloride by these species.[31,32]

^{35}Cl NMR Experiments

The complexation of the Cl^- anion was also studied by ^{35}Cl NMR spectroscopy.[33,34] The ^{35}Cl line width and chemical shift of the Cl^- signal in the presence of **2**-nH^+ were significantly different from those of free Cl^-. Values of $\delta_{obs} = 7.5$ ppm and $\omega_{obs} = 350$ Hz were observed[35] for the chemical shift and the linewidth of the ^{35}Cl NMR signal. The Cl^- anions were in fast exchange between the complexed and the solvated state. Therefore the observed chemical shifts (δ_{obs}) and line widths (ω_{obs}) are related to the chemical shifts and linewidths of the complexed (δ_c and ω_c) solvated (δ_s and ω_s) forms and the fractions (x) of complexed Cl^- anions by equations (*3*) and (*4*).

$$\delta_{obs} = x\delta_c + (1 - x)\delta_s \quad (3)$$

$$\omega_{obs} = x\omega_c + (1 - x)\omega_s \quad (4)$$

We have previously reported the values of 31 Hz for ω_s and 2.9 ppm for δ_s of solvated Cl^- anions in the presence of non-complexing protonated linear polyamines.[34] Assuming a 1/1 binding stoichiometry and 1 : 6 value for the fraction of complexed Cl^-, and using equations (*3*) and (*4*), one calculates values of $\delta_c = 40$ ppm for the contribution of complexation to the ^{35}Cl NMR chemical shift and $\omega_c = 1700$ Hz for the line broadening[35] in D_2O/H_2O:1/9 at pH = 2.5 where compound **2** (2.5×10^{-2} M) remains hexaprotonated. Since ^{35}Cl possesses a nuclear quadrupolar moment, the pronounced increase in linewidth between the solvated and complexed Cl^- anions may be attributed to a non-symmetrical environment of the spherical anion in the complex. These observations are in agreement with the solid state structure of the Cl^- complex with **2**-6H^+. Indeed, the X-ray study revealed that of the six Cl^- anions present in the solid state only C13, interacting with 4 ammonium centres (N2, N3, N5 and N6), was located within the cavity of the macrocycle which adopts a pocket-like conformation. A detailed analysis of the structure showed that the environment around this particular Cl^- atom was somewhat unsymmetrical in the complex (Figure 7).

No ^{35}Cl NMR measurements were performed for binding of Cl^- by **1**-6H^+. However, we have previously found that the 32 membered hexaazamacrocycle differing from **1** only by the number of CH_2 groups bridging the two diethylenetriammonium binding subunits (9 instead of 4), formed dinuclear Cl^- complexes[34,35] (in $MeOH/H_2O$:6/4 solution). This agrees with the structural study above, where the hexaprotonated compound **1** is found to form a dinuclear Cl^- complex in the solid state. Indeed, 2 out of 6 Cl^- anions (C13 and C13″) present in the structure are

located in close proximity to 3 ammonium centres (N1, N2, N3 and N1″, N2″, N3″), one above and the other below the plane of the macrocycle (Figure 3).

Molecular Dynamic Studies. 1-6H$^+$ and 2-6H$^+$ in Computational Phases

The advent of high-speed computers makes it possible to model the behaviour of molecules *in vacuo* or in solution using Monte Carlo (MC) and molecular dynamics (MD) simulations.[36,37] A number of important molecules or ions have now been studied using these techniques, including for example non-polar molecules,[38] various ions,[39] Cl^- ionophores,[40] peptides or proteins.[41] MD simulations have been performed for a wide variety of applications. These include exploring the temporal behaviour of macromolecular systems,[42] determining 3-dimensional structure from NOE-NMR (nuclear Overhauser effects from nuclear magnetic resonance experiments) data,[43] calculating relative free enthalpies of similar systems,[44] and performing crystallographic *R* factor refinements.[45]

Since information about the architecture of molecules **1** and **2** was available from X-ray crystallography, it was of interest to see whether the conformations of these molecules in solution were different from those in the crystalline state. First, an analysis of the intrinsic dynamic behaviour of **1**-6H$^+$ and **2**-6H$^+$ in a dielectric continuum was performed by means of computer molecular dynamics simulations. The solvation and counter ion effects were then taken into account by inclusion of TIP3P model[46] water molecules or Cl^- ions and repeating the molecular dynamics simulations. It is important to point out that these simulation techniques are *computer time intensive*, and that a study of the motion over times longer than a nanosecond is currently prohibitive.[47] Many interesting molecular events are characterized by times longer than nanoseconds, and X-ray coordinates were used as a starting point for the simulations; the molecular dynamics trajectories were correlated to this starting coordinate set and only the phase space close to it was explored.

Computational Technique

The molecular mechanics and dynamics software package AMBER (Assisted Model Building with Energy Refinement[49]) has been used to calculate the energy, optimize the structures, and perform the integration of Newton's equations over time, leading to the simulation of the dynamic behaviour of the macrocycles. The various systems consisted of a hexaprotonated polyamine macrocycle with or without counter ions in water. The solvent was modelled either by using a continuum model or explicitly including the water molecules. The total energy E_T has the form

$$E_T = \Sigma_{bonds} K_r(r - r_{eq})^2 + \Sigma_{angles} K_\Theta(\Theta - \Theta_{eq})^2 + \Sigma_{dihedrals}\, V_n/2(\cos(n\varphi - \gamma)) + \Sigma_{i<j}(A_{ij}/R_{ij}^{12} - B_{ij}/R_{ij}^{6} + q_i q_j/\varepsilon R_{ij})$$

where r, Θ, and φ represent, respectively, the bond length, the bond angle, and the dihedral angle. R_{ij} is the distance between atoms *i* and *j*, q_i the atomic charge on *i*, and ε the dielectric constant. The deformations of bonds r and bond angles Θ from their reference value r_{eq} and Θ_{eq} were treated in the harmonic approximation, and the rotation around dihedral angles was taken into account by Fourier terms. The dielectric constant ε was set to 78.6 when performing simulations without explicit inclusion of the solvent molecules, and to 1.0 when simulating the solute in a water

TABLE VIII

Potential function parameters for bond lengths, bond angles, dihedral angles, non-bonded interactions and charges for both 1-6H$^+$ and 2-6H$^+$. For nomenclature see P.A. Kollman *et al.*, *J. Am. Chem. Soc.*, **106**, 765 (1984). The force field is considered within the united atom approximation.

Bond	K_r	r_{eq} (Å)
C–C	317.0	1.531
C–$N_{protonated}$	367.0	1.513
C–O	450.0	1.384
H–$N_{protonated}$	434.0	1.011

Angles	K_θ	θ_{eq}°
C–C–C	80.0	112.0
C–N–C $N_{protonated}$	80.0	112.0
N–C–C $N_{protonated}$	80.0	110.5
C–O–C	80.0	109.5
O–C–C	80.0	105.5
H–N–H $N_{protonated}$	35.0	109.5
H–N–C $N_{protonated}$	35.0	109.5

Atom	R*	ε
$N_{protonated}$	1.824	0.170
C	2.192	0.118
O	1.723	0.170
H	0.000	0.000
Cl^-	2.479	0.118

Torsion	$V_n/2$	δ	n
X–C–C–X	2.0	0.0	3
X–C–O–X	0.5	0.0	3
X–N–C–X	1.4	0.0	3

Charges					
1-6H$^+$	C(–C–C)	C(–N)†	C(–N)††	N	H(–N)
	0.010	0.300	0.310	−0.300	0.340
2-6H$^+$	C(–N)	C(–O)	N	O	H(–N)
	0.310	0.250	−0.300	−0.500	0.340

† For C atoms in N–C–C–C–C–N. †† For C atoms in N–C–C–N.

box. The CH_2 groups were treated in the united atom approximation;[50] the hydrogen atoms on the nitrogen were included explicitly and treated as point charges without 6–12 van der Waals terms. Parameters used in the simulations and reported in Table VIII were partly taken from the AMBER-OPLS parameter set[51] and partly derived from our force field tests on protonated mono(poly)amines.[52] The simulations including explicitly the solvent were run within a box of TIP3P[53] water with minimum image periodic boundary conditions.[54] In this case the solute–solvent and solvent–solvent interactions were truncated with a residue-based cutoff at 8.5 Å. The bondlengths involving hydrogen atoms in both solute and solvent were kept fixed throughout the simulation using the constraint algorithm SHAKE.[55] The integration

of the equations of motion was done using the Verlet algorithm[56] with a step size 1 fs for simulations in a continuous dielectric, and 2 fs for simulations includi explicit water molecules. Initial velocities for all atoms of the system were taken fr a Boltzmann distribution at 300 K. The simulations were run at a constant tempe ture of 300 K and constant pressure of 10^5 Pa.

The initial coordinates for the systems were the crystallographic coordinates. F the simulation with explicit water, they were prepared by superimposing the mac cycle on the coordinates of an equilibrated TIP3P water box. Water molecules witl 2.5 Å of the solute were discarded. Before determination of MD trajectories, t energy of the starting system was minimized in order to avoid bad local ator contacts.

1-6H$^+$ and 2-6$^+$ in a Continuous Dielectric Medium

The first simulations were performed on the hexaprotonated polyamines **1**-6H$^+$ a **2**-6H$^+$ with the solvent represented as a continuum and without the counter-io The electrostatic interactions were all divided by a factor of 78.6 corresponding to experimental ε of water. The MD trajectories were computed over 50 ps and coordinates saved every ps for averaging.

The evolution of total energy over the 50 ps of the MD run showed that after o 25 ps energetic fluctuations decreased for both **1**-6H$^+$ and **2**-6H$^+$ macrocyc (Figure 8). Averaging of geometrical parameters was done either over the tc simulation time or over the last 25 ps of the MD trajectory.

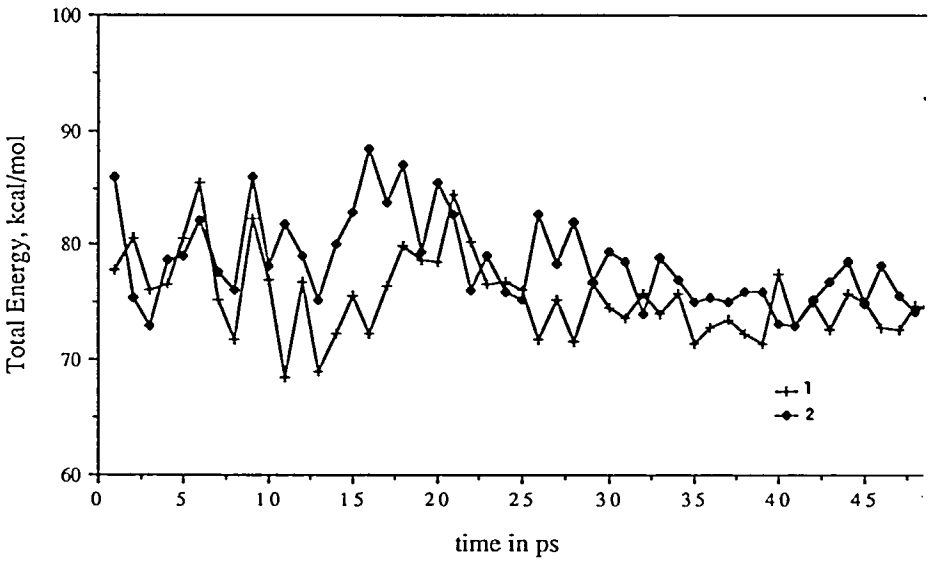

FIGURE 8 History of the total energy over 50 ps of MD of **1**-6H$^+$ and **2**-6H$^+$ in a dielectric contin (ε = 78.6).

For **1**-6H$^+$ slight structural modifications were observed. The relative orientat of the NH_2^+ binding sites were remarkably stable. Indeed, the $^+$N–C–C- dihedral angles remained within the crystallographic orientations: there were *gauche* and two *trans* dihedrals with no dihedral transitions (Figure 9). It

remarkable that the 1-4 $^{+}$N–C–C–N^{+} electrostatic repulsions damped by the dielectric constant of water did not lead to any interconversions. The conformational mobility of the macrocycle was due to small motions around the C–C–C–C and $^{+}$N–C–C–C dihedral angles. The minimum, maximum, mean and root mean square (RMS) deviation values for the four $^{+}$N–C–C–N^{+} dihedral angles are given in Table IX. The mean values obtained from the MD run compare with the standard deviation with the $^{+}$N–C–C–N^{+} dihedral angles from the crystal structure of 66.4 and 173.7° for *gauche* and *trans* dihedrals.

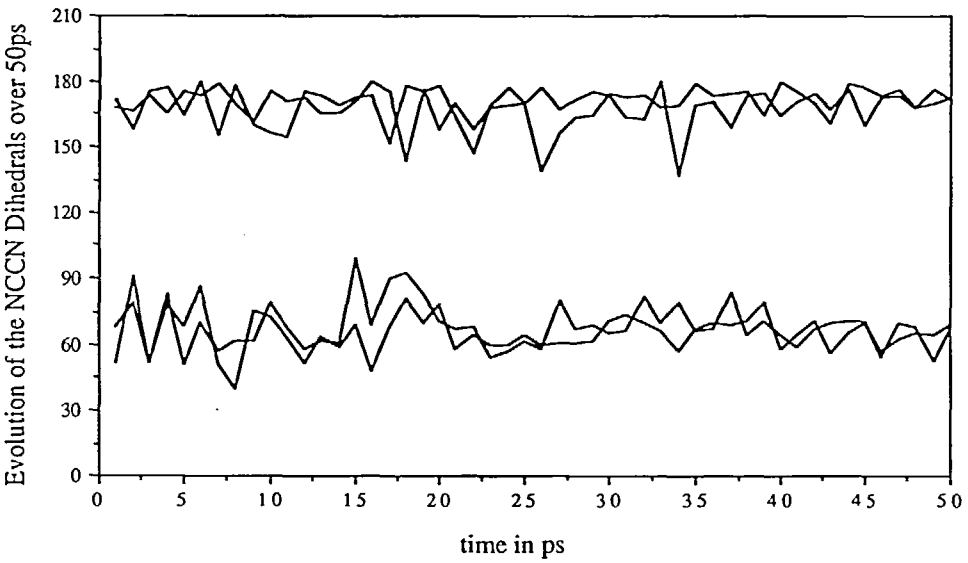

FIGURE 9 History of the $^{+}$N–C–C–N^{+} dihedrals over 50 ps of MD of **1**-6H^{+} in a dielectric continuum (ε = 78.6).

TABLE IX
Descriptive statistics of the NCCN dihedrals of **1**-6H^{+} over 50 ps in a dielectric continuum.

Min-Max	Mean Angle	RMS Deviation
50.1–85.9°	65.4°	8.8°
137.5–180.0°	168.8°	9.1°
51.0–99.2°	68.5°	11.1°
139.2–179.9°	169.5°	8.2°

The analysis of **2**-6H^{+} over 50ps of MD showed that the main feature of the dynamics of this macrocycle in a continuous dielectric without counter-ion effects, was a breathing motion of the "tennis ball seam" shaped structure. The breathing involved coupled displacement of the O and the N "fragments" of the macrocycle (Figure 10), *i.e.*, interconversion of "saddle" shaped structures having alternatively the oxygen atoms or central nitrogen atoms at short distance. Computing the O···O and N···N distances over time (Figure 11) confirmed this observation: the deviation from the mean interatomic distances were comparable for each step (ps), and the distance variations were directly opposite for O···O and N···N. The O···O and N···N mean distances over the 50 steps were respectively 7.80 and 6.93 Å.

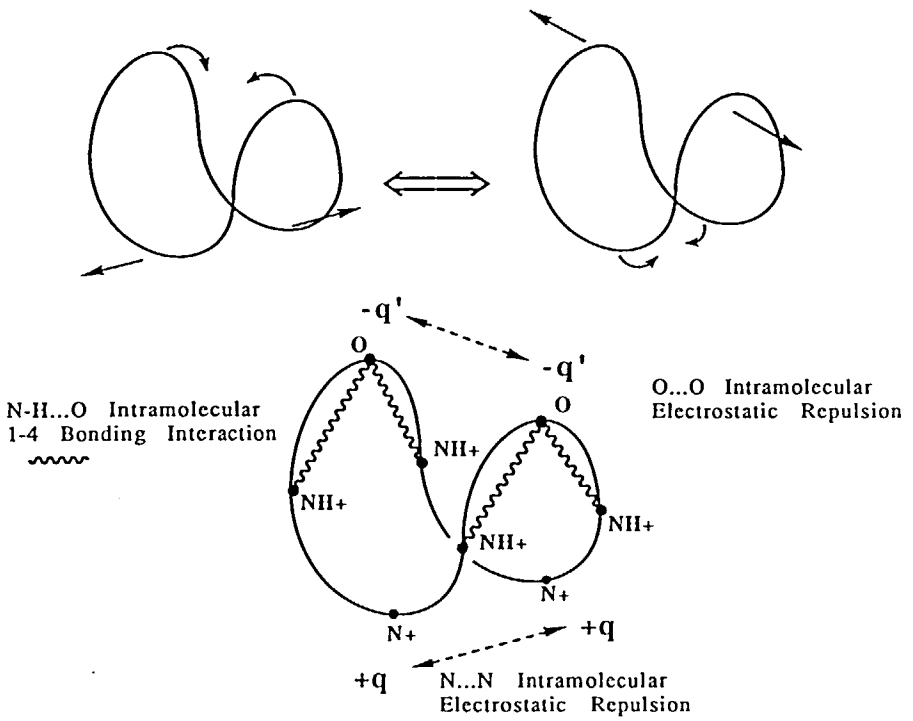

FIGURE 10 Schematic "tennis ball seam" shape and dynamic behaviour of 2-6H$^+$ in a dielectric continuum ($\varepsilon = 78.6$).

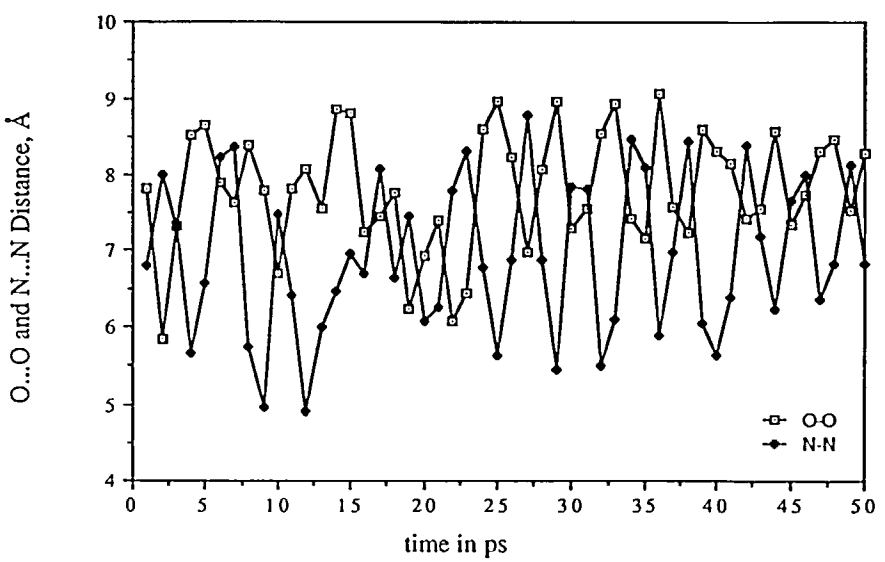

FIGURE 11 O···O and N···N distances over 50 ps of MD of 2-6H$^+$ in a dielectric continuum ($\varepsilon = 78.6$).

Interestingly, the O···O mean distance is longer than the N···N distance of two charged groups which is expected to exert a larger electrostatic repulsion than the O···O interaction.

The overall mobility of the different atoms during MD simulations could be expressed by their root mean square (RMS) distance or position fluctuations calculated over the simulation time: $<\Delta r^2>^{1/2} = <(r_i - <r_i>)^2>^{1/2}$. The RMS fluctuations of the interatomic O···O and N···N distances were respectively about 0.78 and 1.02 Å, and thus the mobility of the central N "fragment" was greater than the mobility of the O ether junction. Along the MD trajectory, the O-C-C-N^+ dihedral angles remained in the *gauche* conformation through 1-4 intramolecular N^+–H···O interactions probably favouring the overall "tennis ball seam" shape of the cycle. There were no bifurcated NH_2^+···O bonds: the N–H···O distances for the two NH_2^+ hydrogens varied in opposite directions. The minimum N–H···O distances varied from 2.17 to 2.99 Å (Table X) and were longer than typical N–H···O hydrogen bonds (about 2.0Å).[57]

TABLE X

Descriptive statistics of the 8 possible intramolecular N–H···O interactions (Å) for **2**-6H$^+$ over 50 ps in a dielectric continuum.

	H1	H1′	H2	H2′	H3	H3′	H4	H4′
Minimum	2.17	2.99	2.36	2.21	2.53	2.32	2.43	2.35
Mean	2.52	3.42	3.16	2.77	3.14	2.85	3.31	2.64
Maximum	3.02	3.88	3.89	3.90	3.84	3.98	3.83	3.33

The mobility of the different atoms expressed by their position (RMS) fluctuations calculated over the simulation time could be compared to the average observed in the crystal using the experimentally determined B thermal factors:[58] $<\Delta r^2>^{1/2} = (3B/8\pi^2)^{1/2}$. The calculated RMS fluctuations in **1**-6H$^+$ and **2**-6H$^+$ were similar and of the order of 0.65 Å for N, C or O atoms; thus their computed B thermal factor of *ca* 11.12 Å^2 was about 4.5 times larger than the B factors obtained from X-ray diffraction experiment.

1-6H$^+$ and 2-6H$^+$ in TIP3P Water

The conformations and dynamics of molecules may be strongly influenced by solvation. The special behaviour of aqueous systems arising from the unique hydrogen bonding properties of water requires its explicit representation in order to understand all properties. The macrocycles **1**-6H$^+$ and **2**-6H$^+$ were surrounded by 600 TIP3P water molecules forming a rectangular box of about $30.0 \times 27.5 \times 23.5$ Å^3. The crystallographic H_2O molecules were not used in the setup. The averaging of the geometrical parameters was done over the last 5ps of the MD simulation in order to avoid artefacts of the first steps of the solvent equilibration. The goals here were to understand the hydration patterns and dynamics of the macrocycles.

Qualitatively, the macrocycle **1**-6H$^+$ did not exhibit any large conformational changes. This result could not be directly derived from the simulation in a continuous dielectric, since water is known to strongly affect conformational preferences of polyamines.[59] Although the short simulation did not allow us to reach definitive conclusions about the effect of solvation on conformational changes, nevertheless the

crystal structure seemed to be rather representative of the structure in water since no dihedral transitions were observed along the MD trajectory. This could be rationalized by the fact that since the NH_2^+ groups in 1-6H$^+$ were partially turned toward the bulk solvent, forming each at least one hydrogen bond with the closest water molecule, there was no driving force for dihedral transitions arising from the presence of the solvent when compared to the solid.

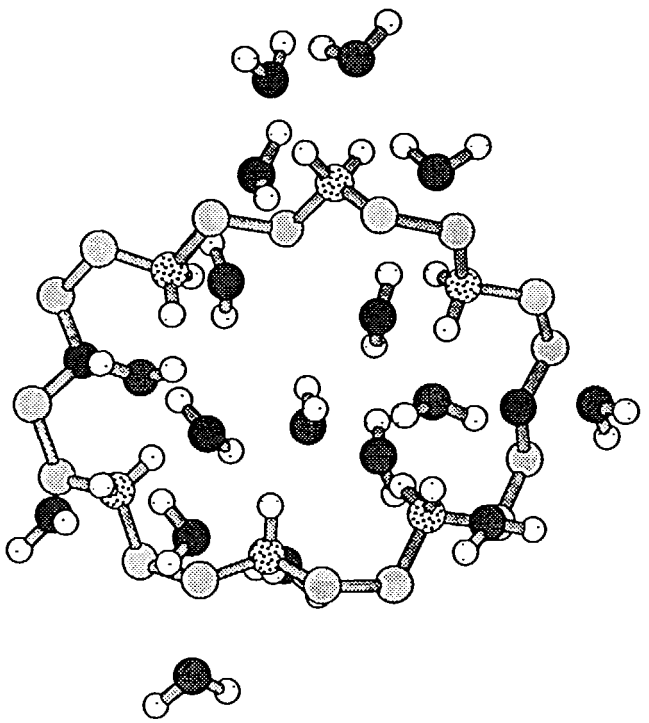

FIGURE 12 Typical water structure surrounding 2-6H$^+$ without counter-ions. The picture is obtained after a 10 ps run of the system at 300 K. Only the water molecules within 2.6 Å are depicted for clarity.

The macrocycle 2-6H$^+$ exhibited more conformational changes during the MD trajectory than 1-6H$^+$. The starting structure was taken from the crystal where NH_2^+ groups were converging toward the centre due to $NH_2^+ \cdots Cl^- \cdots H_2N^+$ interactions. The same conformation without the Cl^- ions seemed not to be compatible with hydration; consequently one NH_2^+ tended to maximize hydrogen bonding with the surrounding solvent by turning both protons toward the bulk solvent within the simulation time (Figure 12). The O–C–C–N$^+$ dihedral angles did not change over 10 ps. The NH_2^+ groups remained in the vicinity of the O-atoms of the ether linkage by means of 1-4 intramolecular interactions. Moreover, H_2O molecules seemed to cooperatively bridge opposite NH_2^+ groups and the O-atom (Figure 13). The overall mobility of the macrocycle decreased on going from the dielectric continuum to TIP3P water, with breathing motions of much lower amplitude. The O$\cdots$O distances in the dielectric continuum and water were respectively about 7.80 and 8.02 Å with RMS of 0.78 and 0.36 Å. The minima and maxima of amplitude in O$\cdots$O distance were respectively 5.85–9.06 and 7.47–

8.75 Å. The fluctuations (RMS) of the O-atoms of the water molecules in both simulations were about 2.0 Å, indicating that, as expected, the solvent molecules exhibited greater mobility than the macrocycles.

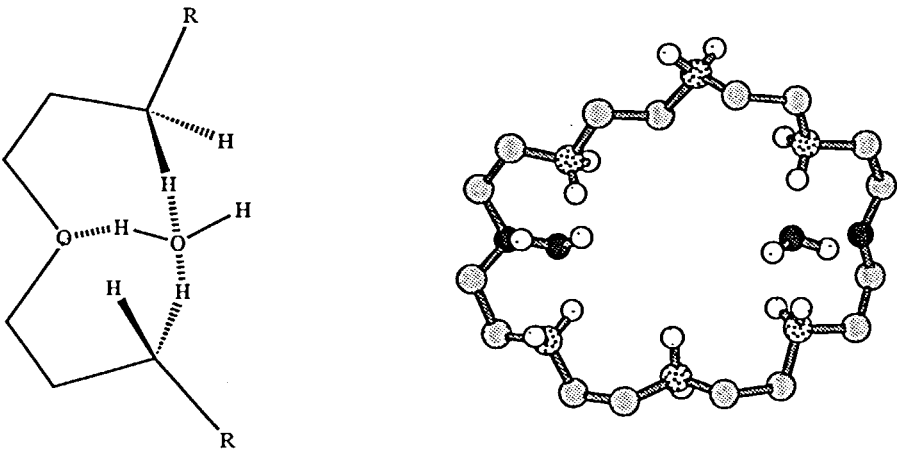

FIGURE 13 Illustration of the cooperative interactions between the NH_2^+ groups, the oxygen atom and water molecules. The structure is the same as in Figure 8 but all except two water molecules have been discarded.

2-6H$^+$ in TIP3P Water with 6 Cl$^-$ Counter-Ions

In order to evaluate the effect of counter-ions on the conformations and hydration of the macrocycle, a simulation with the 6 closest Cl^- ions to one macrocycle 2-6H^+ was run in water. Similarly to the previous MD simulations, the system was run with 600 water molecules. The computation of mean values was done over the last 5 ps of the simulation.

After 10 ps of MD simulation two distinct types of Cl^- ions appeared: 3 Cl^- ions remained in close contact with the macrocycle bridging each two NH_2^+ groups, and 3 other Cl^- ions moving more freely, drifted away from the macrocycle. The $N\cdots Cl^-$ distances of the 3 complexed anions, computed over the last 5 ps, were almost identical for the 6 closest possible interactions, indicating that each Cl^- ion was symmetrically interacting with 2 NH_2^+ groups. The mean $N^+\cdots Cl^-$ distances over 5 ps for the 6 observed interactions ranged from 3.17 to 3.40 Å, and the overall mean $N^+\cdots Cl^-$ distance was about 3.25 Å. The $N^+\cdots Cl^-$ distance fluctuations (RMS) calculated for the 3 Cl^- anions complexed by 2 NH_2^+ ranged from 0.10 to 0.36 Å. These $N^+\cdots Cl^-$ distances computed from the MD simulation were comparable to the distances reported for the crystal structure, and also comparable to similar compounds exhibiting Cl^- complexation; in crystals of a chloride cryptate[22] the $N^+\cdots Cl^-$ distances range from 3.19 to 3.39 Å. The 3 non complexed Cl^- ions diffused in the bulk water and did not remain in close contact with the NH_2^+ groups. Computing the fluctuations of the anions over the last 5 ps of the simulation showed distinctly that among the 3 complexed Cl^- ions having position RMS fluctuations of 0.17, 0.29 and 0.31 Å, the first one is less mobile than the other two. All the "free" Cl^- ions having larger values of position RMS fluctuations (0.48, 0.81 and 0.84 Å) seem to be mobile. Since the time-scale of molecular dynamics

simulations was about 1/1000th of the time scale of NMR measurements, it is difficult to compare directly the results. Nevertheless, the fact that among the complexed Cl^- ions, one had a lower mobility then the other was in good agreement with the ^{35}Cl NMR observation of Cl^- anion binding by **2**-6H$^+$. Furthermore, comparison of the structure in the solid state (Figure 7) and similar conformations obtained throughout the molecular dynamics simulation corroborate that, as in the solid state, one Cl^- anion is tightly bound in solution.

Functional Properties of 1 and 2 in Phosphoryl Transfer Processes

Macrocycles **1** and **2** have been shown to catalyze a variety of phosphoryl transfer processes involving both dephosphorylation (such as ATP hydrolysis) and phosphorylation (*e.g.* synthesis of polyphosphate derivatives).[13,19,20] One of the purposes of the present studies was also to gather information about the way in which **1** and **2** effect these transformations.

Although the conformations found here for the **1**-6H$^+$,2Cl$^-$ and the **2**-6H$^+$,Cl$^-$ species are for the solid state and for a different anion, they may nevertheless have some significance with respect to the structural and mechanistic features involved. Thus, it is worth pointing out that the overall shape of **2**-6H$^+$ (Figures 4–7) gives support to the hypothetical structure drawn previously for the phosphoryl transfer process catalyzed by this same macrocycle.

One could even argue that the relative disposition of the diagonally located central nitrogens in the diethylenetriamine subunits of **1**-6H$^+$ and **2**-6H$^+$ may have some relation to the reaction properties of these species. Indeed, whereas in **1**-6H$^+$ these nitrogen sites (N2, N2′ in Figure 3) are *trans* with respect to the mean plane of the molecule, they are *cis* in **2**-6H$^+$. This might be related to the fact that both molecules catalyze ATP hydrolysis[19] and form a monophosphorylated intermediate[13,19,20] with similar efficiencies, while the "pocket-like" shape of **2**-6H$^+$ would allow for substantial cocatalysis of phosphoryl transfer to a bound susbtrate.[13,20]

Solid state structures of the two fully protonated hexaaza macrocycles **1**-6H$^+$ and **2**-6H$^+$ indicated distinct complexation of Cl^- anions. **1**-6H$^+$ was found to be almost planar, and to interact preferentially with 2 Cl^- anions of 6 present in the crystal (one above and the other below) being thus the first example of a characterized dinuclear Cl^- complex. **2**-6H$^+$ adopted a "pocket-like" or "tennis ball seam" conformation. Although only a macrocyclic system, it formed a well defined inclusion complex with Cl^- by adopting a "pocket" shape, thus generating a pseudocavity. Binding of Cl^- by **2**-6H$^+$ in aqueous solution was also demonstrated by pH-metric as well as ^{35}Cl NMR spectroscopy. The special features of **2**-6H$^+$ were due probably to the CH_2–O–CH_2 linkages that permit intramolecular interactions with NH_2^+ groups and which may induce a locking effect leading to the stabilization of the structure. These observations are further supported by molecular dynamics simulations of the systems. The **1**-6H$^+$ and **2**-6H$^+$ macrocycles exhibited different dynamic behaviour in the absence or presence of solvent. For **1**-6H$^+$ no significant changes were observed in the continuum dielectric or a water box (TIP3P model). However, the **2**-6H$^+$ macrocycle exhibited a marked breathing motion with coupled vibrations of the apical positions of the "tennis ball seam" shaped structure. Explicit water molecules or counter-ions restricted these motions. Solvent molecules interacting cooperatively with several solvation sites, or counter-ions, were critical to stabilize the native structure.

ACKNOWLEDGEMENTS

We would like to acknowledge the University Louis Pasteur and the CNRS (URA 422 and 424 for financial support. We thank the Groupement Scientifique IBM-CNRS for generous allocation of computer time and the Rhône-Poulenc Company for financial support to S.B. G.W. is grateful to the "Région Alsace" for co-financing a Computer Graphics System.

SUPPLEMENTARY MATERIAL

Compound 1: Table S1 : temperature factors for anisotropic atoms; Table S2: hydrogen atoms positional parameters; Table S3: complete set of bond distances; Table S4: complete set of bond angles; Table S5: observed and calculated structure factors amplitudes (*10) for all observed reflections.
Compound 2: Table S6: temperature factors for anisotropic atoms; Table S7: hydrogen atoms positional parameters; Table S8: complete set of bond distances; Table S9; complete set of bond angles; Table S10: observed and calculated structure factors amplitudes (*10) for all observed reflections. All are available from the authors upon request.

REFERENCES

1. J.J.R. Frausto da Silva and R.J.P. Williams, *Struct. Bond.*, **29**, 67 (1976).
2. J.-M. Lehn, *Angew. Chem. Int. Ed. Engl.* **27**, 89 (1988); J.-M. Lehn, *Science*, **227**, 849 (1985); P.G. Potvin and J.-M. Lehn, in *Synthesis of Macrocycles: The Design of Selective Complexing Agents*, R.M. Izatt, J.J. Christensen eds., (J. Wiley and Sons, New York, 1987).
3. J.L. Pierre and D. Baret, *Bull. Soc. Chim. Fr.*, 367 (1983); F. Vögtle, H. Sieger and W.H. Müller, *Topics Curr. Chem.*, **98**, 143 (1981); F.P. Schmidtchen, *Top. Curr. Chem.*, **132**, 101 (1986).
4. N.F. Curtis, *Coord. Chem. Rev.*, **3** 3 (1968); C.K. Poon, *Coord. Chem. Rev.*, **10**, 1 (1973); L.F. Lindoy, *Chem. Soc. Rev.* **4**, 421 (1975); G.A. Nelson, *Coordination Chemistry of Macrocyclic Compounds* (Plenum Press, New York, 1979).
5. K.B. Mertes and J.-M. Lehn in *Comprehensive Coordination Chemistry*, G. Wilkinson, ed. (Pergamon Press, New York, 1987); Y.L. Agnus, in *Copper Coordination Chemistry : Biochemical and Inorganic Perspectives*, K.D. Karlin and J. Zubieta, eds. (Adenine Press, New York, 1983); A.E. Martin and S.J. Lippard, in *Copper Coordination Chemistry : Biochemical and Inorganic Perspectives*, K.D. Karlin and J. Zubieta, eds. (Adenine Press, New York, 1983).
6. B. Dietrich, M.W. Hosseini, J.-M. Lehn and R.B. Sessions, *J. Am. Chem. Soc.*, **103**, 1282 (1981); M.W. Hosseini and J.-M. Lehn, *Helv. Chim. Acta.*, **69**, 587 (1986); E. Kimura, *Top. Curr. Chem.*, **128**, 113 (1985); M.W. Hosseini and J.-M. Lehn, *Helv. Chim. Acta*, **71**, 749 (1988).
7. H.E. Simmons and C.H. Park, *J. Am. Chem. Soc.*, **90**, 2428 (1968).
8. E. Graf and J.-M. Lehn, *J. Am. Chem. Soc.*, **98**, 6403 (1976).
9. R.I. Gelb, B.T. Lee and L.J. Zompa, *J. Am. Chem. Soc.*, **107**, 909 (1985); R.I. Gelb, L.M. Schwartz and L.J. Zompa, *Inorg. Chem.*, **25**, 1527 (1986); F. Peter, M. Gross, M.W. Hosseini and J.-M. Lehn, *J. Electroanal Chem. Interfacial Electrochem.*, **144**, 279 (1983); E. Garcia-Espana, M. Micheloni, P. Paoletti and A. Bianchi, *Inorg. Chim. Acta*, **102**, L9 (1985); M.F. Manfrin, L. Moggi, V. Castelvetro, V. Balzani, M.W. Hosseini and J.-M. Lehn. *J. Am. Chem. Soc.*, **107**, 6888 (1985); D. Heyer and J.-M. Lehn, *Tetrahedron Lett.*, **27**, 5869 (1986).
10. M.W. Hosseini and J.-M. Lehn, *Helv. Chim. Acta*, **70**, 1312 (1987); M.W. Hosseini, A.J. Blacker and J.-M. Lehn, *J. Am. Chem. Soc.*, **112**, 3896 (1990).
11. R.J. Motekaitis, A.E. Martell, J.-M. Lehn and E.I. Watanabe, *Inorg. Chem.*, **21**, 4253, (1982); R.J. Motekaitis, A.E. Martell, B. Dietrich and J.-M. Lehn, *Inorg. Chem.*, **23**, 1588 (1984); R.J. Motekaitis, A.E. Martell, I. Murase, J.-M. Lehn and M.W. Hosseini, *Inorg. Chem.*, **27**, 3630 (1988).
12. A.E. Martin and J.E. Bulkowski, *J. Org. Chem.*, **47**, 415 (1982).
13. M.W. Hosseini and J.-M. Lehn, *J. Am. Chem. Soc.*, **109**, 7047 (1987).
14. J. Comarmond, P. Plumeré, J.-M. Lehn, Y. Agnus, R. Louis, R. Weiss, O. Kahn and I. Morgenstern-Badarau, *J. Am. Chem. Soc.*, **104**, 6330 (1982).

15. P.K. Coughlin, J.C. Dewan, S.J. Lippard, E.I. Watanabe and J.-M. Lehn, *J. Am. Chem. Soc.*, **101**, 265 (1979); P.K. Coughlin and S.J. Lippard, *Inorg. Chem.*, **23**, 1446 (1984); *ibid, J. Am. Chem. Soc.*, **106**, 2328 (1984).
16. R.J. Motekaitis, A.E. Martell, J.-P. Lecomte and J.-M. Lehn, *Inorg. Chem.*, **22**, 609 (1983).
17. R.J. Motekaitis and A.E. Martell, *J. Chem. Soc. Chem. Commun.*, 915 (1988).
18. J.-P. Lecomte, J.-M. Lehn, D. Parker, J. Guilhem and C.J. Pacard, *J. Chem. Soc. Chem. Commun.*, 296 (1983).
19. M.W. Hosseini, J.-M. Lehn, M.P. Mertes, *Helv. Chim. Acta*, **66**, 2454 (1983); *ibid.* **68**, 818 (1985); M.W. Hosseini, J.-M. Lehn, L. Maggiora, K.B. Mertes and M.P. Mertes, *J. Am. Chem. Soc.*, **109**, 537 (1987); G.M. Blackburn, G.R.J. Thatcher, M.W. Hosseini and J.-M. Lehn, *Tetrahedron Lett.*, **28**, 2779 (1987); R.C. Bethell, G. Lowe, M.W. Hosseini and J.-M. Lehn, *Bioorg. Chem.*, **16**, 418 (1988); M.W. Hosseini, J.-M. Lehn, K.C. Jones, K.E. Plute, K.B. Mertes and M.P. Mertes, *J. Am. Chem. Soc.*, **111**, 6330 (1989).
20. M.W. Hosseini, J.-M. Lehn, *J. Chem. Soc. Chem. Commun.*, 1155 (1985); P.G. Yohannes, K.E. Plute, M.P. Mertes and K.B. Mertes, *Inorg. Chem.*, **26**, 1751 (1987); M.W. Hosseini and J.-M. Lehn, *J. Chem. Soc. Chem. Commun.*, 397 (1988).
21. B. Metz, J.-M. Rosalky and R. Weiss, *J. Chem. Soc. Chem. Commun.*, 533, (1976); F.P. Schmidtchen and G. Müller, *J. Chem. Soc. Chem. Commun.*, 1115 (1984).
22. B. Dietrich, J. Guilhem, J.-M. Lehn, C. Pascard and E. Sonveaux, *Helv. Chim. Acta*, **67**, 91 (1989).
23. B. Dietrich, J.-M. Lehn and C. Pascard, *Tetrahedron Lett.*, **30**, 4125 (1989).
24. J. Cullinane, R.I. Gelb, T.N. Margulis and L.J. Zompa, *J. Am. Chem. Soc.*, **104**, 3048 (1982).
25. A. Bianchi, E. Garcia-Espana, S. Mangani, M. Micheloni, P. Orioli and P. Paoletti, *J. Chem. Soc. Chem. Commun.*, 729 (1987); A. Bencini, A. Bianci, P. Dapporto, E. Garcia-Espana, M. Micheloni, P. Paoletti and P. Paoli, *J. Chem. Soc. Chem. Commun.*, 753, (1990).
26. B.A. Frenz, in *Computing in Crystallography*, H. Schenk, R. Olthof-Hazekamp, H. Van Koningveld and G.C. Bassi, eds. (Delft University Press, Delft, 1978).
27. M.S. Lehmann and F.K. Larsen, *Acta Crystallogr.*, **A30**, 580 (1974).
28. G. Germain, P. Main and M.M. Woolfson, *Acta Crystallogr.* **B26**, 274 (1970); G. Germain, P. Main and M.M. Woolfson, *Acta Crystallogr.*, **A27**, 368 (1971).
29. N. Walker and D. Stuart, *Acta Crystallogr.*, **A39**, 158 (1983).
30. D.T. Cromer and J.T. Waber, *International Tables for X-ray Crystallography*, (Kynoch Press, Birmingham, 1976).
31. B. Dietrich, M.W. Hosseini, J.-M. Lehn and R.B. Sessions, *Helv. Chim. Acta*, **66**, 1262 (1983).
32. M.W. Hosseini, *Thèse de Doctorat*, Université Louis Pasteur, Strasbourg, 1983.
33. J.-P. Kitzinger, J.-M. Lehn, E. Kauffmann, J.L. Dye and A.I. Popov, *J. Am. Chem. Soc.*, **105**, 7549 (1983).
34. M.W. Hosseini, J.-P. Kintzinger, J.-M. Lehn and A. Zahidi, *Helv. Chim. Acta*, **72**, 1978 (1989).
35. M.W. Hosseini, J.P. Kintzinger, J.-M. Lehn and A. Zahidi, unpublished results; A. Zahidi, *Thèse de Doctorat*, Université Louis Pasteur, Strasbourg, 1986.
36. C.L. Brooks, M. Karplus and B.M. Pettitt, *Adv. Chem. Phys.*, **71**, 1988.
37. J.A. McCammon and S.C. Harvey, *Dynamics of Proteins and Nucleic Acids*, (Cambridge University Press, Cambridge, 1987).
38. V.G. Dashevsky and G.N. Sarkisov, *Mol. Phys.*, **27**, 1272 (1974).
39. G. Palinkas, W.O. Riede and K. Heinzinger, *Z. Naturforsch*, **32A**, 1137 (1977).
40. G. Wipff, J.-M. Wurtz, *Nouv. J. Chim.*, **13**, 807 (1989); B. Owenson, R.D. McElroy, A. Pohorille *J. Am. Chem. Soc.*, **110**, 6992 (1988). B. Owenson, R.D. McElroy, A. Pohorille *J. Mol. Struct. (Theochem).*, **179**, 467 (1988); T.P. Lybrand, J.A. McCammon, G. Wipff *Proc. Nat. Acad. Sci. USA*, **83**, 833 (1986).
41. P.J. Rossky, M. Karplus, *J. Am. Chem. Soc.*, **101**, 1913 (1979). P. Ahlström, O. Teleman and B. Jönsson, *J. Am. Chem. Soc.*, **110**, 4198 (1988).
42. M. Karplus and J.A. McCammon, *Scientific Am.*, **254**, 42 (1986).
43. L. Nilsson, G.M. Clore, A.M. Gronenborn, A.T. Brunger and M. Karplus, *J. Mol. Biol.*, **188**, 455 (1986).
44. W.F. van Gunsteren and P.K. Weiner, *Computer Simulation of Biomolecular Systems* (Escom, Leiden, 1989).
45. A.T. Brunger, J. Kutiyan and M. Karplus, *Science*, **235**, 456 (1987).
46. W.L. Jorgensen, *J. Am. Chem. Soc.*, **103**, 335 (1981).
47. T.P. Straatsma and J.A. McCammon, *J. Chem. Phys*, **91**, 3631 (1989).
48. S.H. Northrup, M.R. Pear, C.-Y. Lee, J.A. McCammon and M. Karplus, *Proc. Natl. Acad. Sci. U.S.A.*, **79**, 4035 (1982).

49. P.K. Weiner and P.A. Kollman, *J. Comput. Chem.*, **2**, 287 (1981); U.C. Singh, P.K. Weiner, J. Caldwell and P.A. Kollman, AMBER-UCSF 3.0.
50. S.J. Weiner, P.A. Kollman, D.A. Case, U.C. Singh, C. Ghio, G. Alagona, S. Profeta and P. Weiner, *J. Am. Chem. Soc.*, **106**, 765 (1984).
51. W.L. Jorgensen and J. Tirado-Rives, *J. Am. Chem. Soc.*, **110**, 1657 (1988).
52. S. Boudon and G. Wipff, *J. Comp. Chem.*, **12**, 41 (1991).
53. W.L. Jorgensen, J. Chandrasekhar, J.D. Madura, R.W. Impey and M.L. Klein, *J. Chem. Phys.*, **70**, 926 (1983).
54. N. Metropolis, A.W. Rosenbluth, M.N. Rosenbluth, A.H. Teller and E. Teller, *J. Chem. Phys.*, **21**, 1087 (1953).
55. W.F. van Gunsteren and H.J.C. Berendsen, *Mol. Phys.*, **34**, 1311 (1977).
56. L. Verlet, *Phys. Rev.*, **159**, 98 (1967).
57. G.C. Pimentel and A.D. McClellan, *The Hydrogen Bond*, (Freeman, San Francisco, 1960).
58. B.T.M. Willis and A.W. Pryor, *Thermal Vibrations in Crystallography*, (Cambridge University Press, Cambridge, 1975).
59. S. Boudon and G. Wipff, *J. Mol. Struct. (THEOCHEM)*, in press.